Valence proton-neutron interactions throughout the mass surface

D. S. Brenner,[1,2] R. B. Cakirli,[2,3] and R. F. Casten[2]
[1]*Clark University, Worcester, Massachusetts 01610, USA*
[2]*Wright Nuclear Structure Laboratory, Yale University, New Haven, Connecticut 06520, USA*
[3]*Department of Physics, University of Istanbul, Istanbul, Turkey*
(Received 19 December 2005; published 21 March 2006)

Empirical average proton-neutron interaction energies, δV_{pn}, between the last nucleons can be isolated using double differences of masses. We have examined the systematic behavior of δV_{pn} throughout the mass surface using the 2003 mass table that includes many new and improved experimental masses. The results are especially revealing for self-conjugate nuclei and in regions of strong shell closures in heavy nuclei. In the former the large *p-n* interaction strength can be interpreted as a consequence of the $T = 0$ interaction between protons and neutrons in spatially similar orbitals. In the latter, the bifurcated systematic can be understood in terms of the evolution of proton and neutron orbital overlaps in regions surrounding a shell closure. In regions between shells, anomalies are sometimes encountered that are not fully understood. They might reflect structural effects or could arise from one or more erroneously measured masses. A scheme based on fractional shell filling is presented that may serve as a signature of shell structure in exotic nuclei. A link between empirical *p-n* interactions and growth rates of collectivity is pointed out. Finally, our analysis is used to identify candidates for future mass measurements and their needed levels of accuracy, many of which will require new exotic beam facilities.

DOI: 10.1103/PhysRevC.73.034315 PACS number(s): 21.30.Fe, 21.10.Dr, 21.60.Ev, 27.60.+j

I. INTRODUCTION

The total binding energy of the nucleus, derived from atomic masses, embodies the sum of all nucleonic interactions. Differences of masses or binding energies, such as two-nucleon separation energies and Q_α values, provide signatures of shell closure and, in some cases, the onset of deformation. Other constructs have been designed to isolate specific nucleonic interactions. One of these, a double difference of masses (binding energies), designated δV_{pn}, has been used to isolate the average empirical proton-neutron (*p-n*) interaction energy [1–3]. It has long been recognized that the *p-n* interaction is responsible for nuclear deformation and the evolution of collective behavior with changing N and Z [4–6]. Thus, a detailed mapping of δV_{pn} throughout the mass surface might reveal nuances as nuclear structure evolves through regions of shape and phase transitions.

For even-even nuclei, the average *p-n* interaction of the last two protons with the last two neutrons can be defined [1,2,7] as

$$\delta V_{pn}^{ee}(Z,N) = 0.25[\{B(Z,N) - B(Z,N-2)\} - \{B(Z-2,N) - B(Z-2,N-2)\}], \quad (1)$$

where B is the binding energy of the nucleus. As has been discussed previously [1,7], assuming that the nuclear core remains essentially unchanged, δV_{pn}, by its definition, largely cancels the interactions of the last nucleons with the core. A given δV_{pn} value for an even-even nucleus refers to the interaction of the $(Z-1)^{\text{th}}$ and Z^{th} valence protons with the $(N-1)^{\text{th}}$ and N^{th} neutrons.

The empirical interaction strength of the last proton with the last neutron, in the case with Z odd and N even is

$$\delta V_{pn}^{oe}(Z,N) = 0.5[\{B(Z,N) - B(Z,N-2)\} - \{B(Z-1,N) - B(Z-1,N-2)\}] \quad (2)$$

and similarly for an odd-neutron nucleus [3]. Hereafter we drop the superscript and parenthetical notation and refer to the interaction as δV_{pn}.

About 15 years ago δV_{pn} values of even-even nuclei were investigated and showed dramatic singularities for nuclei with $Z = N$ and considerably smaller irregularities near shell closures, although only a few δV_{pn} values could be extracted in the latter regions. Recently, Audi, Wapstra, and Thibault published [8] an updated atomic mass evaluation that includes entries for many new nuclei and more precise data for many masses previously known. The new masses, in turn, give rise to many more δV_{pn} values in regions where structural changes occur, such as near closed shells. This wealth of new data prompted us to reconsider the systematics of δV_{pn} throughout the mass surface and to do so for odd A nuclei as well as even-even ones. The results of our analysis are the subject of this article. A letter highlighting some of our findings has been published recently [9,10] and another has been submitted [11].

II. $Z = N$ NUCLEI

δV_{pn} values for light nuclei show especially large interaction strengths when $Z = N$. This feature was discussed in Ref. [2] and attributed primarily to the $T = 0$ component of the interaction. This conclusion was supported by both schematic and realistic shell-model calculations. Later it was shown by Van Isacker, Warner, and Brenner [3] that these enhancements can be understood with Wigner's SU(4) symmetry [12] where qualitative agreement was found between the empirical δV_{pn} values and the predictions of unbroken SU(4) symmetry for *p*-shell nuclei. Others have proposed alternate interpretations [13]. For the *sd*-shell sizable deviations from simple SU(4) predictions were found that were attributed to the spin-orbit interaction that, together with the Coulomb repulsion,

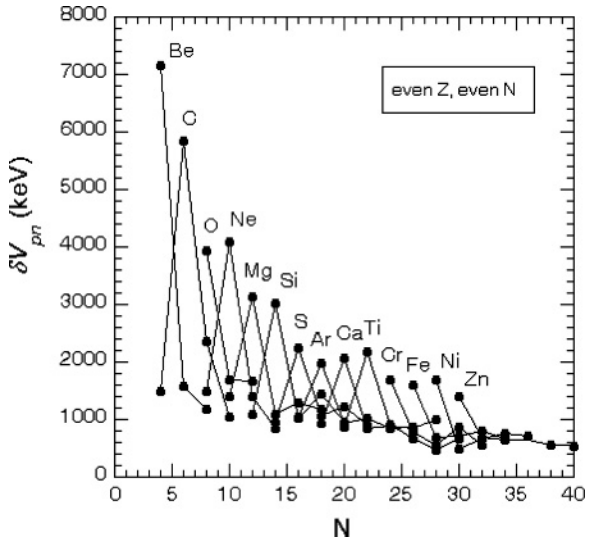

FIG. 1. δV_{pn} values in the region of self-conjugate, $Z = N$, nuclei. Empirical δV_{pn} values are negative (the empirical *p-n* interaction is predominantly attractive). For simplicity, here and in the following figures, we show $|\delta V_{pn}|$. Only masses based on experimental data from Ref. [8] are used to compute δV_{pn} and only values with errors <50 keV are shown.

increases in importance with A and break the SU(4) symmetry. This manifests itself as a decrease in δV_{pn} for $Z = N$ nuclei with increasing A. Reference [3] went on to speculate, however, that a *pseudo*-SU(4) symmetry might be restored in the *pf*-shell leading to a reversal of this trend. Therefore, it is of interest to extend the systematics of δV_{pn} for self-conjugate nuclei to higher Z to see if the δV_{pn} strength is restored.

Figure 1 shows the δV_{pn} values for even-even light nuclei. Only δV_{pn} values with errors <50 keV are shown and only masses based on experimental data are considered in computing δV_{pn}. Values for self-conjugate nuclei up to $Z = 30$ (Zn), the start of the *pf* shell, are known. If one wishes to test the *pseudo*-SU(4) hypothesis, however, mass measurements of very exotic nuclei are needed so that extraction of δV_{pn} values can be determined deeper into the shell. A list of masses required to extend the systematics to Zr ($Z = 40$) is found in Table I. Measurements with errors in the range of 100–200 keV should suffice in this region and may be feasible at existing facilities.

TABLE I. Suggestions for future mass measurements.

Region of interest	To compute δV_{pn}	Mass measurements needed[a]
Self-conjugate	^{64}Ge	^{62}Ge(u)
	^{68}Se	^{66}Se(u)
	^{72}Kr	^{70}Kr(u)
	^{76}Sr	^{74}Sr(u)
	^{80}Zr	^{80}Zr(1490), ^{78}Zr(u)
$N \sim 50$	^{72}Zn	^{70}Ni(350)
	^{74}Zn	^{72}Ni(440), ^{70}Ni(350)
	^{84}Se	^{82}Ge(240)
	^{86}Se	^{84}Ge(u), ^{82}Ge(240)
	^{95}Zr,^{97}Mo	^{95}Zr(2.4)
	^{97}Zr,^{99}Mo	^{97}Zr(2.8)
$N \sim 82$	^{118}Cd	^{116}Pd(60)
	^{120}Cd	^{118}Pd(210), ^{116}Pd(60)
	^{122}Cd	^{122}Cd(40), ^{120}Pd(120), ^{118}Pd(210)
	^{124}Cd	^{124}Cd(60), ^{122}Cd(40), ^{122}Pd(u), ^{120}Pd(120)
	^{126}Cd	^{126}Cd(50), ^{124}Cd(60), ^{124}Pd(u), ^{122}Pd(u)
	^{125}In, ^{126}Sn	^{124}Cd(60), ^{122}Cd(40)
	^{128}Sn	^{126}Cd(50), ^{124}Cd(60)
	^{130}Sn	^{128}Cd(290), ^{126}Cd(50)
	^{132}Sn	^{130}Cd(280), ^{128}Cd(290)
	^{134}Sn	^{134}Sn(100), ^{132}Cd(u), ^{130}Cd(280)
	^{152}Nd	^{150}Ce(50)
$N \sim 126$	^{200}Pt	^{198}Os(u)
	^{202}Pt	^{202}Pt(u), ^{200}Os(u), ^{198}Os(u)
	^{204}Hg	^{202}Pt(u)
	^{206}Hg	^{204}Pt(u), ^{202}Pt(u)
	^{209}Pb	^{207}Hg(150)
	^{210}Pb	^{208}Hg(u)
	^{211}Pb	^{209}Hg(u), ^{208}Hg(u)
	^{212}Pb	^{210}Hg(u), ^{208}Hg(u)
	^{225}Ra	^{223}Rn(u)
	^{227}Ra	^{225}Rn(u), ^{224}Rn(u)

[a]The uncertainty of the experimental mass in keV is shown in parentheses. If the mass is unknown, the designation is (u). Data taken from Ref. [8].

III. SHELL EFFECTS

A. $N \sim 126$ region

Figure 2 (top) shows the δV_{pn} values for for Pb and TI even-even nuclei near ^{208}Pb. As neutrons are added beginning at $N{\sim}100$ δV_{pn} values diverge into two trends, one decreasing, one increasing. Beyond $N = 126$ the δV_{pn} values of the lower branch abruptly jump in magnitude to a level comparable to that of the upper branch before the shell closure, about 300 keV. This pattern of behavior was discussed in Refs. [9,11] in terms of shell structure near doubly magic nuclei where correlations and collective effects are less important than elsewhere. We summarize that discussion below.

For nuclei near the top of the $Z = 50$–82 shell the last protons occupy low-j, high-n shell-model states. A similar pattern is found near the top of the $N = 82$–126 shell where the last neutrons also occupy low-j, high-n orbitals. Because of the high spatial overlap of the similar proton and neutron orbitals, the short-range residual interaction among valence particles is strong.

The lower branch, in contrast, exhibits decreasing *p-n* strength in the same region. These nuclei have $Z > 82$ and $N < 126$; the protons here are filling high j, low-n orbitals, whereas the neutrons are occupying the low-j, high n orbitals found at the end of the $N = 82$–126 shell. As a consequence the spatial overlap of the proton and neutron orbitals is diminished and is reflected by lower δV_{pn} values. Once N exceeds 126, the valence neutrons enter spatially similar states to the protons

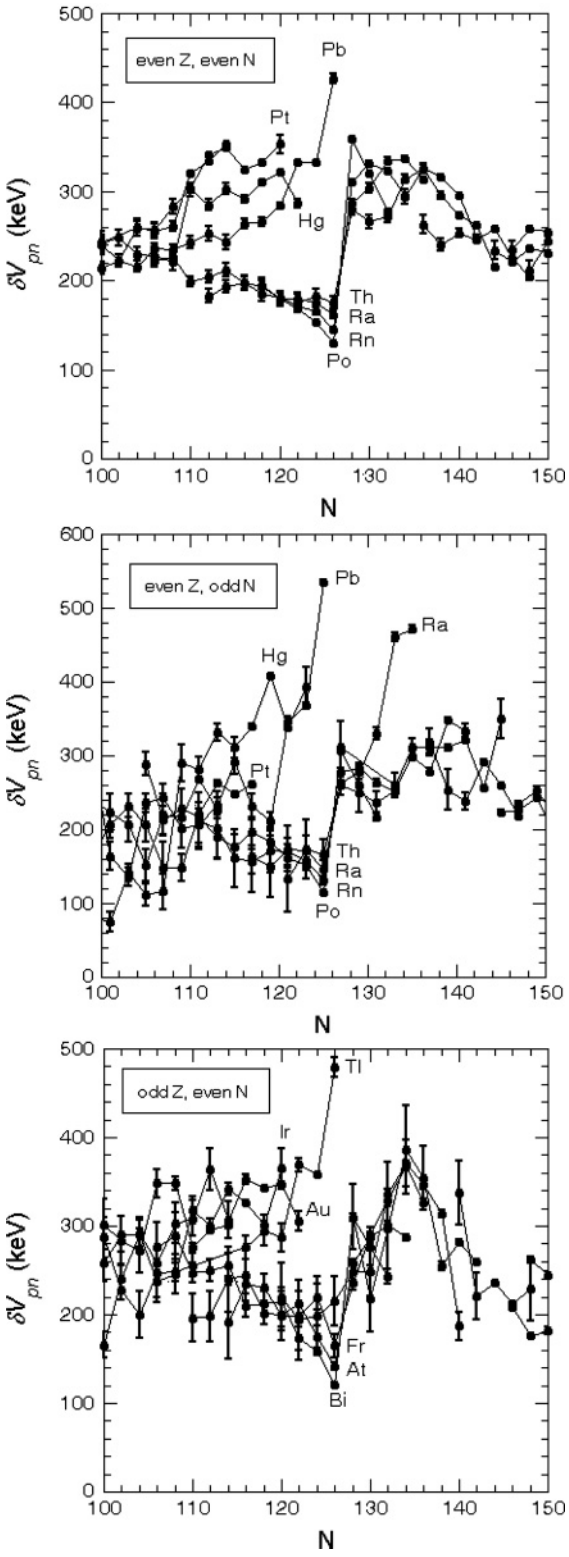

FIG. 2. (Top) δV_{pn} values for even-even nuclei near ^{208}Pb. (Middle and bottom) Similar to the top panel but for even-Z, odd-N nuclei and odd-Z, even-N nuclei, respectively.

and a strong p-n interaction results. This effect beyond $N = 126$ can be seen in the jump in δV_{pn} for Po, Rn, Ra, and Th nuclei in Fig. 2 (top).

Odd-A nuclei exhibit similar behavior. Figure 2 (middle) shows δV_{pn} values for even Z, odd N nuclei in this region. Again a bifurcation occurs with increasing N near the shell closure followed by a coalescence at $N = 126$. Also note that the Ra isotopes with $N = 133$, 135 have anomalously large δV_{pn} values as compared with the general trend. Figure 2 (bottom) displays the systematic for odd-Z, even-N nuclei that exhibits the same divergence and convergence as found for the other cases. Also note that there appears to be a local maximum for δV_{pn} at $N = 135$, similar but less distinct than that noted for the odd-A Ra isotopes. This feature is discussed in Sec. IV B of this article.

B. $N \sim 82$ region

It is interesting to examine the δV_{pn} systematic in the vicinity of another well-established shell. Figure 3 shows data near the $N = 82$ shell closure for even-Z, even N, and odd-A nuclei. Indeed, the Sn and In isotopes exhibit patterns similar to that seen for Pb/Tl near $N = 126$ (Fig. 2). The even-even and odd-A panels show an increase in δV_{pn} values for Sn/In with increasing N, relative to other elements, below the $N = 82$ shell closure. Recall that we expect larger δV_{pn} values when the last protons and neutrons are filling similar orbits and smaller values when they are not. Let us see if this simple idea can account for variations in δV_{pn} values in this region.

It is instructive to summarize the systematic of the ground-state spins of odd-Z and odd-N nuclei in this region $49 \leqslant Z \leqslant 55$, $73 \leqslant N \leqslant 85$). For $Z = 49$ (In) the valence protons occupy the $1g_{9/2}$ state. Beyond the proton shell closure at $Z = 50$ (Sb, I, Cs isotopes) the last proton is usually in the $2d_{5/2}$ or $1g_{7/2}$ state with the latter preferred as N increases toward, and beyond, 82. Therefore, it is reasonable to conclude that the minor variations in the ground-state proton orbitals are not likely to account for the divergence in δV_{pn} values seen in Fig. 3 near the neutron shell closure.

The even-Z, odd-N ground-state spins, however, suggest a possible explanation. For Cd, Te, Xe, and Ba, $Z = 48$, 52, 54, and 56, respectively, the ground state is either $1/2^+$ or $3/2^+$ up to the neutron shell closure. The overlaps between these low-spin neutron orbitals and $5/2^+$ or $7/2^+$ proton orbitals is expected to be roughly constant and should result in relatively constant δV_{pn} values in this region below the neutron shell closure at $N = 82$. For $N > 82$ the neutrons begin filling the $2f_{7/2}$ state and δV_{pn} is expected to increase significantly because of the similarity of the proton and neutron orbitals occupied, $7/2^+$ and $7/2^-$, respectively. This is consistent with the increases seen in the δV_{pn} values for these nuclei beyond the shell closure.

The divergence of the Sn and In δV_{pn} values from the other nuclei can be understood by considering the evolution of the ground-state spins of Sn isotopes in this region. The lighter odd-A Sn isotopes have either $1/2^+$ or $3/2^+$ ground states. Then for $N = 73$, 75, 77, the Sn ground state becomes $11/2^-$, reverting to $3/2^+$ for $N = 79$, 81. Recall that the last protons in Sn are in a $9/2^+$ state. One would expect a much greater overlap of the $9/2^+$ proton orbital and the $11/2^-$ neutron orbital than for the $9/2^+$ proton and low-spin neutron orbitals.

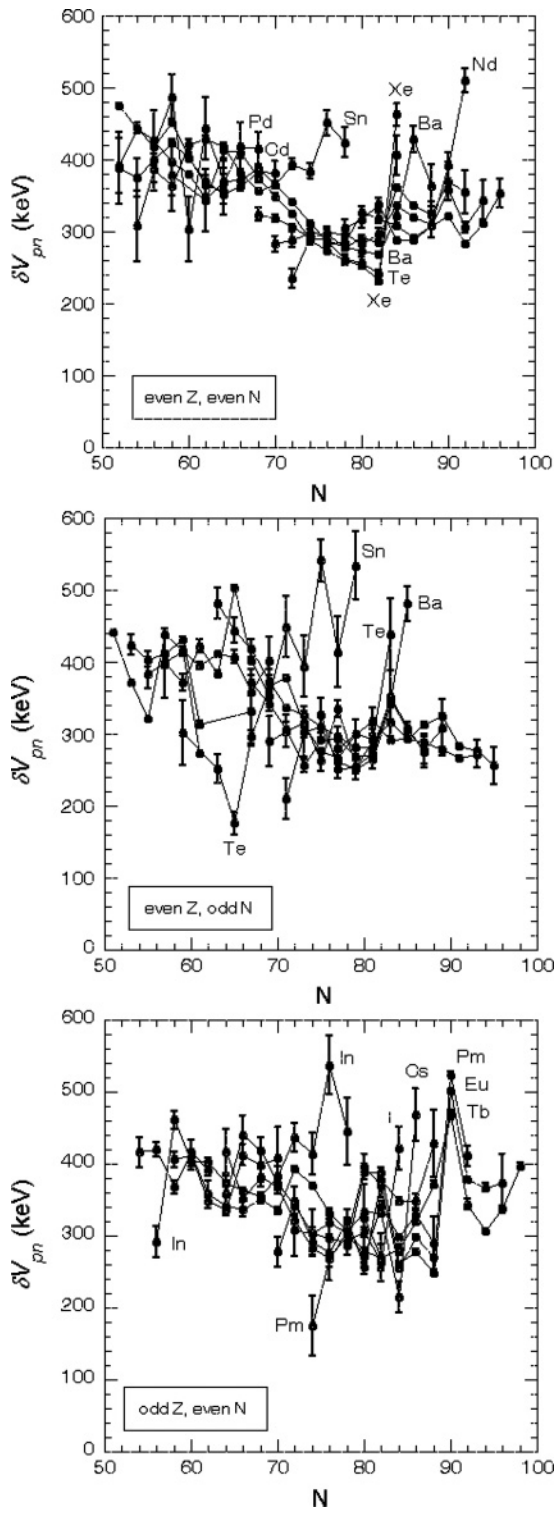

FIG. 3. (Top) δV_{pn} values for even-even nuclei near ^{132}Sn. (Middle and bottom) Similar to the top panel but for even-Z, odd-N nuclei and odd-Z, even-N nuclei, respectively.

This, in turn, could give rise to enhanced δV_{pn} values for Sn and In nuclei with $N = 73$–78. The pattern of δV_{pn} values in Fig. 3 is consistent with this expectation. At $N = 80$ and beyond, δV_{pn} for Sn should be similar to that of Te, Xe, and Ba.

It would be quite interesting to extend the systematic of δV_{pn} for Cd to higher neutron numbers because the Cd ground states for $N = 73, 75, 77$, are $3/2^+$, in contrast to $11/2^-$ for Sn. The orbital overlap conjecture suggests that these Cd isotopes would have δV_{pn} values similar to Te, Xe, and Ba and smaller than the Sn isotopes. The mass measurements needed to extend the Sn and Cd δV_{pn} systematic in this region are listed in Table I.

There are also curiosities that should be noted. Just above the shell closure the Te, Cs, Xe, and Ba isotopes show sharp increases in δV_{pn}. In the case of Ba, δV_{pn} peaks at $N \sim 86$; for the others, the data are lacking at this N. In addition, the odd-Z, even-N data show a dramatic spike at $N = 90$. Te also exhibits anomalous behavior around $N = 65$ in Fig. 3 (middle) and there is an outlying Nd point at $N = 92$ in Fig. 3 (top). The source of these anomalies is not clear. All the masses involved are known with high precision so these were not included in Table I where candidates for new measurements are listed. Discussion of these features, which may or may not be related to structural changes, is found in Sec. IV B.

C. $N \sim 50$ region

Figure 4 shows the δV_{pn} systematic for $N = 35$–70, a region of complex behavior. Let us begin by discussing the spike in δV_{pn} found for Kr and Sr at $N = 50$ as compared to Zr and Mo. Just below $N = 50$ neutrons are filling the $1g_{9/2}$ orbital; beyond they begin occupying the $2d_{5/2}$ state. Protons, in contrast, are filling the $2p_{3/2}$, $1f_{5/2}$, and $2p_{1/2}$ orbitals until Mo, where filling of the $1g_{9/2}$ orbital begins. If our simple orbital overlap concept is considered one would expect a smooth variation in δV_{pn} with rather low values up to $N = 50$ for Kr, Sr, and Zr because protons are filling low-j orbitals and the neutrons are filling a high-j orbital; hence spatial overlap is expected to be modest. In contrast, the valence protons in Mo occupy the same shell-model orbital as the neutrons so an enhanced δV_{pn} is expected, which is clearly not the case. Rather the opposite behavior occurs. Certainly either the qualitative spatial overlap idea fails in this region or the orbit occupations are quite different than given by a simple orderly filling of shell-model states, or, in cases of unstable nuclei, there are mismeasured masses.

Another region of unusual behavior is in the vicinity of $N = 56$. Here there is an apparent spike in δV_{pn} for Sr and Zr and a negative spike for Mo that are difficult to understand. Approaching $N = 56$ the neutrons are filling the $2d_{5/2}$ orbital. For Sr and Zr the protons are filling the $1f_{5/2}$ and then the $2p_{1/2}$ orbitals. Furthermore, the evolution of structure in this region is complex. The Sr, Zr, and Mo nuclei are thought to have relatively low-lying deformed intruder bands, whereas ^{96}Zr has a double subshell closure [14]. Again, one should not expect a simple picture of overlaps of single-proton and -neutron orbitals to adequately describe a region where there is a rapid evolution of structure and where configuration mixing is often significant.

Other anomalies appear in the odd-A nuclei. For example, at $N = 39$ Kr and Sr show a large positive spike in δV_{pn} and Zn a negative one (Fig. 4, middle). Also ^{101}Zr has a large δV_{pn}. For the odd-Z nuclei (Fig. 4, bottom there are apparent anomalies for ^{85}Nb, ^{89}Br, ^{101}Nb, ^{99}Y, and ^{101}Y.

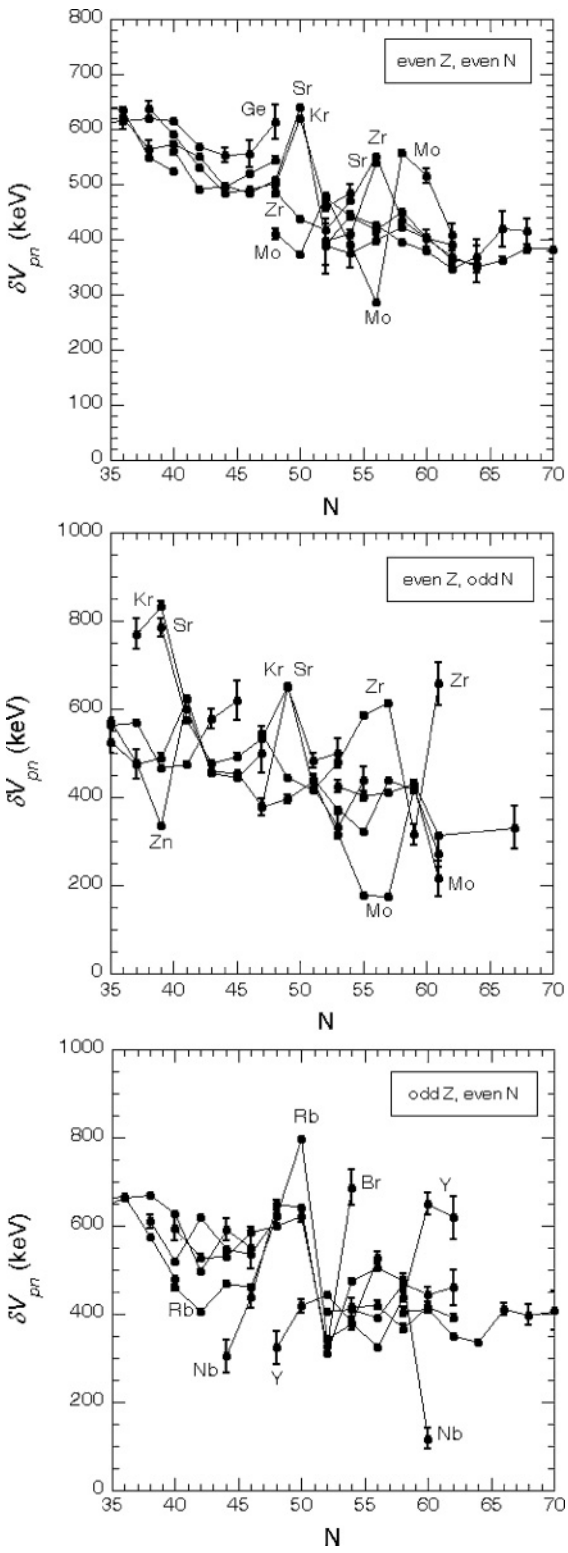

FIG. 4. (Top) δV_{pn} values for even-even nuclei near $N\sim50$. (Middle and bottom) Similar to the top panel but for even-Z, odd-N nuclei and odd-Z, even-N nuclei, respectively.

Clearly, as just noted, the simple qualitative arguments used to explain the evolution of δV_{pn} values in the $N = 82$ and 126 regions are inadequate in regions where structure evolves rapidly with N and Z and where extensive configuration mixing is expected. Rather, what are needed in such regions are microscopic approaches that take into account the complexities of the valence particle interactions. It would be interesting to carry out shell-model calculations in at least some of these regions to see if well-established interactions and model spaces can account for δV_{pn} values that cannot be easily explained by simple overlap arguments involving single-proton and -neutron configurations.

Finally, one should note that the error bars associated with δV_{pn} values are, in general, quite small, reflecting high precision in the mass data. However, it is possible that one or more mass measurements, although, precise, could be incorrect and thus give rise to erroneous δV_{pn} values for multiple nuclei because one mass is involved in four adjacent δV_{pn} values. Sometimes, because the same mass enters the expressions for δV_{pn} with opposite signs, the positive and negative deviations from the general systematic trend in the region can be used to identify likely candidates for erroneous masses. For example, consider the four apparently anomalous points for Zr and Mo at $N = 55, 57$ (Fig. 4, middle). The δV_{pn} values for ^{95}Zr and ^{97}Mo both incorporate the masses of ^{95}Zr and ^{94}Zr but with opposite signs. If ^{95}Zr were less bound by about 400 keV, or, conversely, ^{94}Zr more bound by the same amount, the effect would be to lower δV_{pn} for ^{95}Zr by 200 keV, and raise it for ^{97}Mo by 200 keV completely eliminating the $N = 55$ anomaly. However, an adjustment of the ^{94}Zr mass also affects four even-even δV_{pn} values raising the δV_{pn} values of ^{94}Zr and ^{98}Mo by 100 keV while lowering those of ^{96}Zr and ^{96}Mo by the same amount. The impact on the even-even δV_{pn} systematic is to collapse the positive Zr and negative Mo spikes seen at $N = 56$ in Fig. 4 (top) while introducing new spikes at $N = 54$. In contrast, variation of the ^{95}Zr mass affects only the even-Z, odd-N δV_{pn} values (Fig. 4, middle) for Zr and Mo at $N = 55$.

The δV_{pn} values for ^{97}Zr and ^{99}Mo are linked in a similar way by the masses of ^{97}Zr and ^{96}Zr. Of course the anomalies could also be modified by adjusting both shared masses, but in opposite directions. Other regions where positive and negative spikes in δV_{pn} of similar magnitude occur could be explained in an analogous manner. For the $N = 55, 57$ cases, because the masses of stable ^{94}Zr and ^{96}Zr are likely correct, new measurements of the masses of ^{95}Zr and ^{97}Zr might resolve the matter.

IV. SHAPE TRANSITION REGIONS

A. Deformed rare-earth region

Figure 5 (top) displays the δV_{pn} systematic for the rare-earth region. As N increases there is an evolution in structure from spherical shape through a region of softness to stable quadrupolar deformation at about $N = 92$. Beyond $N = 92$, δV_{pn} values increase for each isotopic chain in parallel fashion such that δV_{pn} for a nucleus (Z, N) is comparable to that for nuclei with $(Z + 2, N + 2)$, $(Z + 4, N + 4)$, etc. For the neutron-rich nuclei of Er-W beyond $N \sim100$, the pattern is broken with a decrease in δV_{pn}.

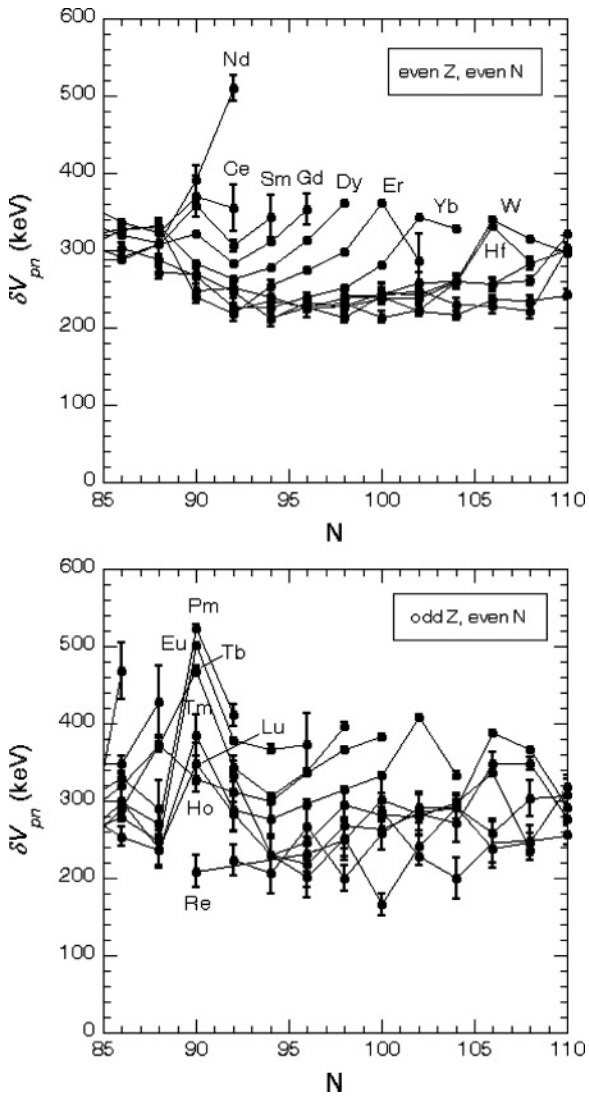

FIG. 5. (Top) δV_{pn} values for even-even nuclei in the rare-earth region. (Bottom) Similar to the top panel but for odd-Z, even-N nuclei.

This curious behavior can be understood qualitatively in terms of the overlaps between proton and neutron Nilsson orbitals in which the down- or up-sloping dependence of the orbital energy on deformation is related to the angle of the orbital plane around the nucleus. Thus, qualitatively, protons and neutrons in orbitals with similar inclination (projection) to the symmetry axis should overlap more than in the case of quite different orbital planes. Because the proton numbers in this region are near midshell, their Nilsson orbit energies tend to be relatively flat as a function of deformation. The neutrons are occupying the first half of the $N = 82$–126 shell and hence their orbit inclinations vary from down sloping for lower N values to flatter near $N = 100$. Thus the proton-neutron orbit overlaps should increase with N for a given Z, as suggested by the δV_{pn} values. Also, addition of pairs of protons and neutrons in tandem places both types of valence particles in orbitals that evolve in slope in a similar way resulting in comparable δV_{pn} values for nuclei with successively increasing Z and N. This should give the kind of parallel slopes in the δV_{pn} values seen in Fig. 5. Of course, this qualitative explanation needs to be backed up by explicit microscopic calculations.

The evolution in nuclear structure and shape between spherical closed shells and deformed spheroids has often been characterized as a phase transition. Recently, Iachello [15] proposed a model for understanding nuclear phase-shape evolution near or at the critical point of a first-order phase transition. In his model the critical point is designated by a special analytic solution called X(5). Specific signatures for X(5) nuclei were predicted and examples of nuclei that fit the X(5) description (e.g., ^{152}Sm, ^{150}Nd) have been found in the $N = 90$ region [16,17]. It is perhaps interesting to examine Fig. 5 (top) to see if there is any unusual variation in δV_{pn} at $N = 90$. Indeed there is a small (approximately 100 keV) divergence of δV_{pn} values, with Ce, Nd, and Sm having enhanced strength relative to Dy and higher Z nuclei. Gd falls intermediate between the two groupings. Odd-Z, even-N nuclei (Fig. 5, bottom) also show enhancements of δV_{pn} for the lower Z nuclei (Pm, Eu, and Tb) at $N = 90$. It is not at all clear if this feature is related to the first-order phase transition postulated for X(5) nuclei. This region is rich in complexity: The disappearance of the $Z = 64$ subshell gap at $N = 90$ or the appearance of an apparent deformed subshell gap at $Z = 66$ are but two factors that may perturb structure and δV_{pn}. Although the variation in δV_{pn} values does not point to a clear structural interpretation, the spike at $N = 90$ is an apparent indicator of change in structure. Finally, note that the δV_{pn} value for ^{152}Nd (Fig. 5, top) is anomalously high. We have no explanation for this but will return to this point at the end.

B. The Ra puzzle

As noted in the $N = 126$ section above, there are interesting features in Fig. 2 (middle, bottom) in the region near $N = 133$–135. Figure 2 (bottom) shows a coherent peak in δV_{pn} values at $N = 134$. Even more curious are the strongly enhanced δV_{pn} values for ^{133,135}Ra visible in Fig. 2 (middle). Figure 6

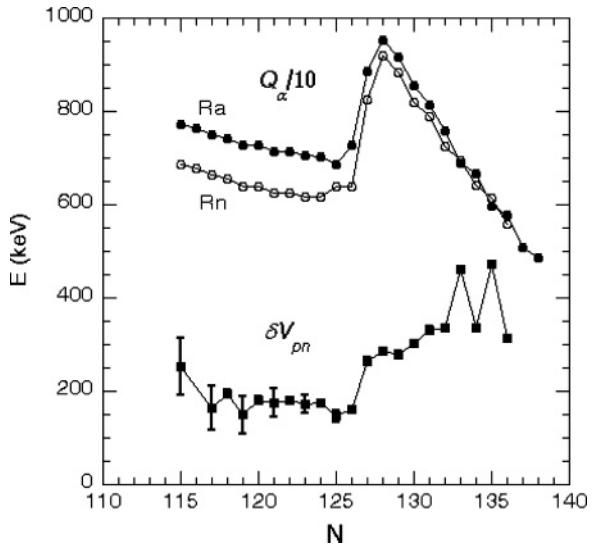

FIG. 6. δV_{pn} values for Ra isotopes and Q_α/10 for Rn and Ra isotopes.

illustrates this more dramatically. Here we plot δV_{pn} for all Ra isotopes together with Q_α values for Ra and Rn divided by 10. The exceptional δV_{pn} values for ^{133,135}Ra are obvious. Also, note that the anomalies are manifested in the Q_α systematics by crossings, although much less dramatic, for Ra and Rn at $N = 133$ and 135. It is not at all surprising that the Q_α and δV_{pn} both show anomalous features as both involve mass differences of Ra and Rn isotopes. The mass data in this region appear to be quite sound as they are derived from α-decay measurements that are usually reliable and have high precision. Assuming the masses are correct, we can speculate on a structural feature that could give rise to anomalously strong δV_{pn} values. One possibility is that δV_{pn} might sense the softness to octupole deformation known in this region. Strong octupole correlations are thought to arise when pairs of orbits that have $\Delta l = \Delta j = 3$ lie close in energy. In this region the couplings are $(1i_{13/2}\text{-}2f_{7/2})$ and $(1j_{15/2}\text{-}2g_{9/2})$, which are close to the Fermi surface for $Z = 88$ and $N = 134$, respectively [18,19]. This occurs exactly at the location of the δV_{pn} anomalies. If *softness* to deformation is indeed detected by δV_{pn}, then one might also associate the peak observed at $N = 90$ in the rare-earth region with this property.

V. FRACTIONAL SHELL FILLING

We have discussed examples, especially in the Pb region, in which the variations in δV_{pn} can be understood in terms of overlaps of proton and neutron wave functions. Away from closed shells toward midshell, such a simple approach cannot work because of extensive configuration mixing. However, we know that in heavy nuclei, the normal parity orbits in a shell begin with orbits having low-n, high-j quantum numbers and end with high-n, low-j quantum numbers. As mentioned before and in Ref. [9] δV_{pn} values will be large if the last protons and neutrons are filling orbits with large spatial overlap. Therefore, even in cases where the simple arguments usable near closed shells are not applicable, δV_{pn} values should be largest if protons and neutrons are filling their representative shells to similar positions. That is, δV_{pn} should be correlated with the fractional filling of proton and neutron shells. For the rare-earth region, the fractional filling for protons and neutrons, which depends on shell size, can be written as follows:

$$f_p = \frac{N_p}{32} \quad \text{and} \quad f_n = \frac{N_n}{44}, \tag{3}$$

where N_p and N_n are the numbers of protons (or neutrons) after the closed shell, whereas 32 and 44 are possible maximum nucleon numbers in the shells, respectively. The idea of correlating δV_{pn} with f_p and f_n is illustrated in Fig. 7 (top). As seen there, the largest δV_{pn} values are indeed along the diagonal line where protons and neutrons occupy similar orbitals and the differences in n and l values for the last protons and neutrons, Δn and Δl, are small. Smaller δV_{pn} values are seen toward the upper left of the diagonal line where protons and neutrons do not occupy similar orbitals, and Δn and Δl values are larger. Of course, this simple picture will be modified by the specific location of the unique parity orbit in each shell. Clearly, data in the lower right part (neutron rich nuclei) would be valuable.

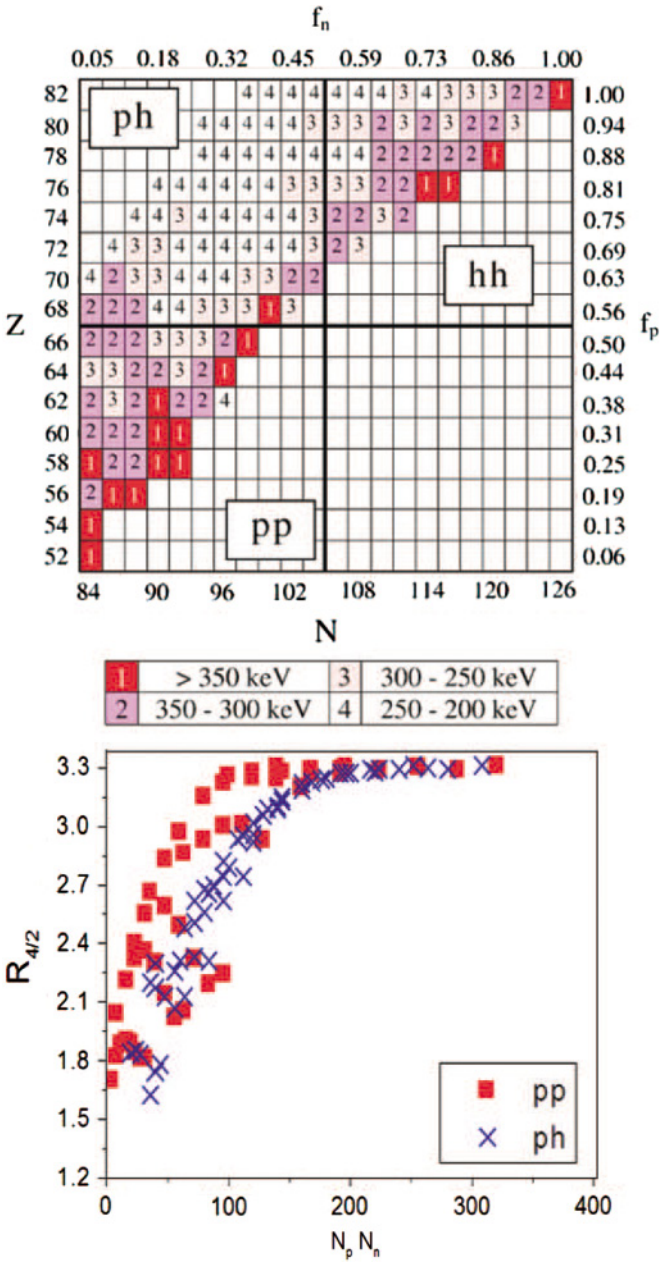

FIG. 7. (Color online) (Top) Empirical δV_{pn} values as a function of both (Z, N) and f_p and f_n, the fractional filling for the $Z = 50$–82, $N = 82$–126 shells. All δV_{pn} values with errors less than 125 keV are shown. Shading gives the magnitude of δV_{pn}. (Based on Refs. [9,11]). (Bottom) $R_{4/2}$ systematic against $N_p N_n$ for particle-particle (pp) ($Z = 50$–66, $N = 82$–104) and particle-hole (ph) ($Z = 68$–82, $N = 82$–104) regions. (Based on Ref. [11].)

Empirical δV_{pn} values depend on the orbits occupied as seen by the specific patterns in δV_{pn} values for the $Z = 50$–82 and $N = 82$–126 shells in Fig. 7 (top). Far from stability, however, shell structure may change for neutrons because of their loose binding and changes in the shape of the mean field. In fact, the 82 and 126 magic numbers may change for exotic nuclei.

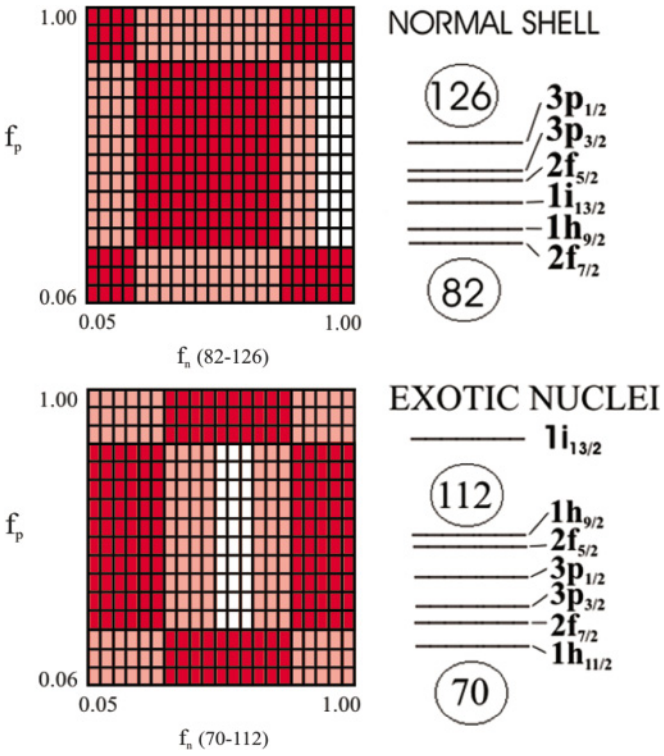

FIG. 8. (Color online) Calculated δV_{pn} values using a δ function interaction [20], for two different assumptions of the order of filling of the neutron shell. Darker shading corresponds to larger δV_{pn} values. (Top) Protons and neutrons with normal shell ordering ($Z = 50$–82, $N = 82$–126). The neutron shell is shown at the right. (Bottom) Scenario for neutron-rich nuclei that have 70–112 magic numbers, whereas protons are filling the same orbits as on the top. The ordering of the neutron orbits is shown at the right.

If the neutron potential becomes more diffuse, the highest l orbits may be near the top and bottom of the shell and a nested pattern of j values may develop as suggested by Ref. [20]. To illustrate this effect for neutron rich nuclei, we use a toy model in Fig. 8 in which a δ function is used to calculate p-n interactions [21]. Although this is not realistic for actual orbits in heavy nuclei, it illustrates the idea involved. The top part of Fig. 8 shows the calculated δV_{pn} values assuming protons and neutrons fill the $Z = 50$–82 and $N = 82$–126, shells in normal order. As a model for the kind of sequence that might be encountered in exotic neutron-rich nuclei we use the sequence suggested in Ref. [20]. This gives new neutron magic numbers 70, 112 instead of 82, 126, whereas protons have the same shell as in Fig. 8 (top) with 50 and 82. The new, calculated δV_{pn} values are shown in Fig. 8 (bottom). The patterns in the two parts of the figure are very different, showing the potential for using δV_{pn} values as a signature of structure in exotic nuclei.

Finally, another interesting aspect of these δV_{pn} values concerns their relation to the growth, and growth rates, of collectivity. Figure 7 (bottom) shows empirical $R_{4/2}$ values against $N_p N_n$ for particle-particle (pp) and particle-hole (ph) nuclei in the rare-earth region. It is clear, as pointed out by Brenner [22] and McCutchan [23], that the pp nuclei have larger $R_{4/2}$ values than ph nuclei for a given $N_p N_n$ until saturation is reached when $R_{4/2}$ goes to 3.33. This means that collectivity grows faster in the pp than in the ph region. If the valence p-n interaction is indeed the primary driving force in generating configuration mixing and collectivity, this effect should be visible in δV_{pn} values. Figure 7 (top) indeed shows exactly the same behavior. The pp region has larger δV_{pn} values than the ph region. Moreover, this is a natural consequence of the fractional filling idea just described; δV_{pn} values are large when protons and neutrons are filling like regions, small in unlike regions. Thus these two figures have the same physical underpinning and are the first direct empirical link between the behavior of nuclear collectivity and empirical valence p-n interaction strengths.

VI. FUTURE MASS MEASUREMENTS

The 2003 mass table has allowed us to investigate the systematic variation of the average valence p-n interaction in regions of the mass surface that previously were poorly known or, in some cases, completely inaccessible. Many tantalizing patterns were revealed, some of which have been rationalized by qualitative arguments based on the attractive nature of the p-n interaction and the overlap of valence nucleon orbitals. As is usually the case, more questions have been raised than answered, which provides an incentive for future mass measurements and for microscopic theory.

In regions of structural change where interesting features of the δV_{pn} systematic are found, additional mass measurements are also desirable. Although four masses are involved in determining δV_{pn}, often only a single mass measurement is needed. The missing or poorly known mass, however, is invariably that of the nucleus furthest from stability and therefore the most challenging to measure. With the exception of self-conjugate nuclei, δV_{pn} values span a range of 150–200 keV in any given region. Thus, in most regions, meaningful trends in δV_{pn} can be discerned only if the errors in individual masses are $\sim$30 keV or better. This requirement has implications for the design of future experiments and the facilities needed to produce the exotic nuclei. In many cases, measurements by trapping techniques are called for. However, for self-conjugate nuclei, the spikes at $Z = N$ in Fig. 1 represent anomalies of the size of a megaelectron volt or more. Here, mass measurements to an accuracy of 100–200 keV might be sufficient. Such measurements can be efficiently made in storage ring experiments. An excellent review of trapping and storage ring techniques has been published by Lunney, Pearson, and Thibault [24].

Table I contains a list of candidates for future mass measurements organized by region of the mass surface as discussed in this article. Most entries are for nuclei known to be bound. In some cases masses have been measured but the precision is poor. For instance, the Cd and Pd nuclei in Table I all have errors in excess of 40 keV, often considerably in excess. Precise masses for these nuclei would be useful in better defining the δV_{pn} systematic for the upper branch approaching the $N = 82$ shell closure. This, in turn, will more stringently test whether our simple orbital overlap idea, that

was so successful in the $N = 126$ region, is valid for the lower shell. Note that the measurement of a single mass (e.g., ^{122}Cd) can often provide useful information for more than one δV_{pn} value. Last, in the ^{208}Pb region, note that a measurement of the mass of ^{208}Hg would give the first δV_{pn} value in the lower right quadrant of Fig. 7.

VII. CONCLUSION

We have surveyed the systematic variation in δV_{pn}, a quantity derived from four masses, that extracts an average empirical proton-neutron interaction strength. The new 2003 mass table that includes many new and improved experimental masses was used for the calculations. The results are especially interesting for self-conjugate nuclei, in regions of strong shell closures, and in regions where shape transitions occur. Near closed shells the splitting of the systematic into two branches was explained in terms of the evolution of proton and neutron orbital overlaps. Orbital overlaps were also invoked to explain the pattern of δV_{pn} variation found for the deformed rare-earth nuclei. Enhanced δV_{pn} values near $N = 90$ and $N = 134$ were identified. These appear to be associated with transition regions where nuclei are *soft* with respect to change in shape; spherical-to-prolate deformed and/or spherical-to-octupolar deformed. Anomalies were noted and discussed. These may reflect subtle structural features or could be because of incorrect masses. A scheme based on fractional shell filling was developed that may serve as a signature of shell structure for unexplored regions that will be accessible at the next generation exotic beam facilities. Another interesting possibility could arise if masses of extremely neutron-rich nuclei with neutron skins could be measured. In such nuclei a decoupling of the outermost neutrons from a proton-neutron core is expected and this might lead to greatly reduced proton-neutron overlaps. As microscopic models for neutron skin nuclei are developed, this hypothesis can be evaluated. Because masses will be one of the first (and only) observables measurable at the limits of isotope accessibility, measurements to obtain δV_{pn} values might be one of the sensitive experimental signatures of the development of a neutron skin. Finally, a list of candidates for future mass measurements was presented.

ACKNOWLEDGMENTS

We are grateful to K. Heyde, J.-Y. Zhang, K. Blaum, and N. Pietralla for helpful discussions and to K. Heyde for providing calculations of p-n interactions with a δ interaction. This work was supported by the U.S. DOE under grants DE-FG02-88ER40417 and DE-FG02-91ER40609.

[1] J.-Y. Zhang, R. F. Casten, and D. S. Brenner, Phys. Lett. **B227**, 1 (1989).
[2] D. S. Brenner, C. Wesselborg, R. F. Casten, D. D. Warner, and J.-Y. Zhang, Phys. Lett. **B243**, 1 (1990).
[3] P. Van Isacker, D. D. Warner, and D. S. Brenner, Phys. Rev. Lett. **74**, 4607 (1995).
[4] I. Talmi, Rev. Mod. Phys. **34**, 704 (1962).
[5] K. Heyde, P. Van Isacker, R. F. Casten, and J. L. Wood, Phys. Lett. **B155**, 303 (1985).
[6] P. Federman and S. Pittel, Phys. Lett. **B69**, 385 (1977); **B77**, 29 (1978).
[7] J.-Y. Zhang *et al.*, in *Proceedings of the International Conference on Contemporary Topics in Nuclear Structure Physics, Cocoyoc, Mexico, Book of Abstracts* (unpublished) C **65**, p. 109 (1988).
[8] G. Audi, A. H. Wapstra, and C. Thibault, Nucl. Phys. **A729**, 337 (2003).
[9] R. B. Cakirli, D. S. Brenner, R. F. Casten, and E. A. Millman, Phys. Rev. Lett. **94**, 092501 (2005).
[10] R. B. Cakirli, D. S. Brenner, R. F. Casten, and E. A. Millman, Phys. Rev. Lett. **95**, 119903(E) (2005).
[11] R. B. Cakirli and R. F. Casten, submitted.
[12] E. Wigner, Phys. Rev. **51**, 106 (1937).
[13] W. Satula, D. J. Dean, J. Gary, S. Mizutori, and W. Nazarewicz, Phys. Lett. **B407**, 103 (1997).
[14] H. Mach, G. Molnár, S. W. Yates, R. L. Gill, A. Aprahamian, and R. A. Meyer, Phys. Rev. C **37**, 254 (1988).
[15] F. Iachello, Phys. Rev. Lett. **87**, 052502 (2001).
[16] R. F. Casten and N. V. Zamfir, Phys. Rev. Lett. **87**, 052503 (2001).
[17] R. Krücken, B. Albanna, C. Bialik, R. F. Casten, J. R. Cooper, A. Dewald, N. V. Zamfir, C. J. Barton, C. W. Beausang, M. A. Caprio, A. A. Hecht, T. Klug, J. R. Novak, N. Pietralla, and P. von Brentano, Phys. Rev. Lett. **88**, 232501 (2002).
[18] R. K. Sheline, Phys. Lett. **B197**, 500 (1987).
[19] W. Nazarewicz, P. Orlanders, I. Ragnarsson, J. Dudek, G. A. Leander, P. Möller, and E. Ruchowsa, Nucl. Phys. **A429**, 269 (1984).
[20] J. Dobaczewski and W. Nazarewicz, Phil. Trans. R. Soc. London A **356**, 2007 (1998); W. Nazarewicz, Nucl. Phys. **A654**, c195 (1999).
[21] K. Heyde, private communication.
[22] D. S. Brenner, J. Radioanalytical Nucl. Chem. **243**, 31 (2000).
[23] E. A. McCutchan, private communication.
[24] D. Lunney, J. M. Pearson, and C. Thibault, Rev. Mod. Phys. **75**, 1021 (2003).